



HAL
open science

Development of a new type shock tube without a diaphragm for gas-dynamic laser research

S. Kugimiya, K. Ichizono, S. Nourgostar, K.N. Sato, S. Kawasaki, Triam
Exp.Group

► **To cite this version:**

S. Kugimiya, K. Ichizono, S. Nourgostar, K.N. Sato, S. Kawasaki, et al.. Development of a new type shock tube without a diaphragm for gas-dynamic laser research. 2004. hal-00001978

HAL Id: hal-00001978

<https://hal.science/hal-00001978>

Preprint submitted on 25 Oct 2004

HAL is a multi-disciplinary open access archive for the deposit and dissemination of scientific research documents, whether they are published or not. The documents may come from teaching and research institutions in France or abroad, or from public or private research centers.

L'archive ouverte pluridisciplinaire **HAL**, est destinée au dépôt et à la diffusion de documents scientifiques de niveau recherche, publiés ou non, émanant des établissements d'enseignement et de recherche français ou étrangers, des laboratoires publics ou privés.

Development of a new type shock tube without a diaphragm for gas-dynamic laser research

S.Kugimiya¹⁾, K.Ichizono¹⁾, S.Nourgostar¹⁾, K.N.Sato²⁾, S.Kawasaki²⁾, TRIAM Exp.Group²⁾

¹⁾Interdisciplinary Graduate School of Engineering Sciences, Kyushu University

²⁾Research Institute for Applied Mechanics, Kyushu University

1.Introduction

A non-diaphragm type shock tube is being developed for the gas-dynamic laser research. The shock tube of this type has been designed to be operated without a diaphragm which the conventional shock tube has in order to separate the high and low pressure regions. By this new scheme, several advantageous properties are expected to be obtained. The vacuum vessel of the conventional shock tube should be opened to atmosphere every time after each shot in order to replace a diaphragm by a new one. This process always introduces impurities into the vacuum vessel. The reproducibility of experiments sometimes depends on the reproducibility of diaphragm-breaking-phenomena. In the non-diaphragm type shock tube, there is no necessity for replacing a diaphragm after each experiment. Thus, it will be possible to reduce influx of impurities in the experiment. In addition, the reproducibility and the efficiency of experiments may be expected to be largely improved.



Fig.1 Photograph of the non-diaphragm type shock tube.

2. High pressure driven pistons in the non-diaphragm shock tube

High pressure driven pistons in the non-diaphragm shock tube are shown in Fig.2. The cylinder sections C and D are filled with a higher pressure gas than that of the driver room. Since a small pinhole ($\phi=1\text{mm}$) is drilled at the center of the piston B, the pressures of cylinder sections C and D are equal at the initial stage. When the gas is released from the C part through exhaust valve, the pressure of section C quickly decreases. Because of a low conductance through the pinhole between C and D, a pressure imbalance quickly develops and this will lead

the fast movement of the piston B toward left hand side. When the gas in the section D flows out through lateral holes, the pressure imbalance between the section D and the driver section causes a fast movement of the piston A to the left side, and this makes the high pressure gas in the driver section flowing into the driven section. Consequently, a shock wave will occur.

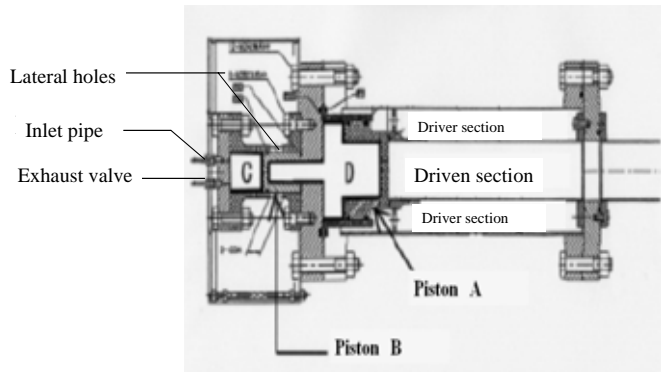


Fig.2 High pressure driven pistons in the non-diaphragm shock tube.

3. Improvement of piston B

At the first stage of the experiment, due to the heaviness and the large lateral area of the piston B, its movement toward the cylinder section C was not so fast to generate the shock wave. Therefore, in order to solve this problem, the new lighter piston which has almost four times smaller surface area was made. Moreover, to increase the gas release speed from the cylinder section C, the exhaust pipe diameter was enlarged. And the lateral holes of the cylinder section C were increased. Finally, after these improvements, shock wave has been generated.



Fig.3 Piston B
(Before improvement)

Table 1. Improvement point

Improvement point	Before improved	After improved
Piston weight g	272	198
Piston surface area cm ²	193	40.9
Lateral hole	2	4
Exhaust pipe diameter(mm)	4	10



Fig.4 Piston B
(After improvement)

4. Measurement of shock wave velocity

Figure 5 shows schematic diagram of the shock tube and instrumentation. The distance between the channel 1 and the channel 2 is 50cm. These two piezo electric detectors pick up shock wave impacts, so we can determine the shock wave velocity by measuring the time interval of these two arrival times of a shock wave. Figure 6 shows waveforms of the piezo electric detectors by arriving a shock wave. By using Rankine–Hugoniot equation, it is possible to calculate the temperatures behind the incident and reflected shock waves from the Mach number.

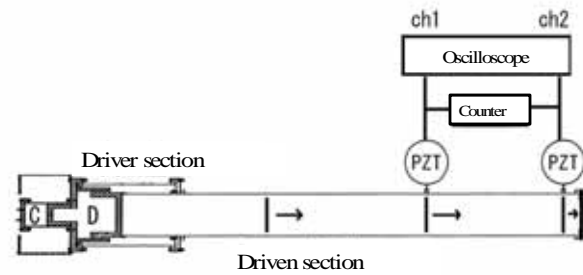


Fig.5 Schematic diagram of the shock tube and instrumentation

The value P_4/P_1 is the initial pressure ratio. T_2 is the temperature behind a incident shock wave, and T_5 is the temperature behind a reflected shock wave. The gas in driver section is He, and the gas in driven section is N_2 . The values of κ_1 and κ_4 are the specific heat ratio of N_2 ($\kappa_1=1.404$) and He ($\kappa_4=1.667$). The values of a_1 and a_4 are the sound speed of N_2 ($a_1=346\text{m/s}$) and He ($a_4=997\text{m/s}$). M_s is the mach number and $T_1(293\text{K})$ is room temperature .

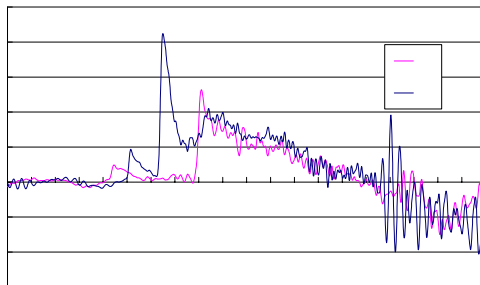


Fig.6 Waveforms of the 1st and 2nd channel piezo electric detectors by arriving a shock wave

$$\frac{P_4}{P_1} = \frac{2\kappa_1 M_s^2 - (\kappa_1 - 1)}{\kappa_1 + 1} \left[1 - \frac{\kappa_4 - 1}{\kappa_1 + 1} \frac{a_1}{a_4} \left(M_s - \frac{1}{M_s} \right) \right]^{\frac{2\kappa_4}{\kappa_4 - 1}}$$

$$T_2 = \frac{[2\kappa_1 M_s^2 - (\kappa_1 - 1)](\kappa_1 - 1)M_s^2 + 2}{(\kappa_1 + 1)^2 M_s^2} T_1$$

$$T_5 = \frac{[2(\kappa_1 - 1)M_s^2 + (3 - \kappa_1)](3\kappa_1 - 1)M_s^2 - 2(\kappa_1 - 1)}{(\kappa_1 + 1)^2 M_s^2} T_1$$

5. Experimental result

Figure 7 shows mach number versus initial pressure ratio P_4/P_1 . M_{sth} is theoretical values from Rankine–Hugoniot equation. In this experiment, driver section and driven section pressure range were 5~20atm, and 5~20Torr respectively, and obtained mach number was in the range of 2.45~4.11. When P_1 was 5Torr, mach number uncertainty was $\pm 0.01 \sim 0.14$. When P_1 was 10Torr,

it was $\pm 0.01 \sim 0.13$. When P_1 was 20 Torr, it was $\pm 0.01 \sim 0.03$. From this result, reproducibility was better in the case of $P_1=20$ and higher initial pressure ratio P_4/P_1 .

The theoretical value is determined by assuming that the gas in driver section instantaneously flows into the driven section. However, in the experiment this flow is actually restricted by piston operation, which produces a delay time to start the operation.

Figure 8 shows temperatures behind incident shock wave T_2 , and Fig. 9 shows temperatures behind reflected shock wave T_5 . The value of T_2 is in the range of 600~1200K, and T_5 is in the range of 1000~2500K.

6. Summary

Before the modification of the structure in high pressure region, shock wave could not be generated. However, after modification, shock wave has successfully been generated. Reasonable reproducibility has been achieved and stable high pressure driven piston operation has been established.

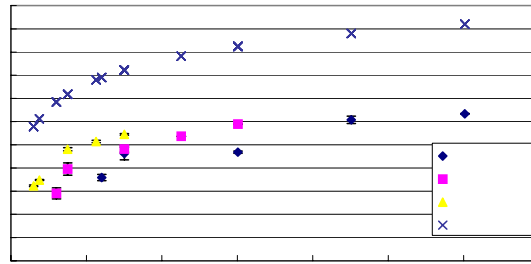


Fig. 7 Mach number as a function of initial pressure ratio P_4/P_1 .

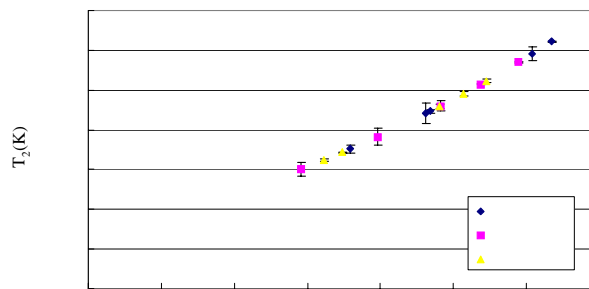


Fig. 8 Temperatures behind incident shock wave T_2 as a function of Mach number.

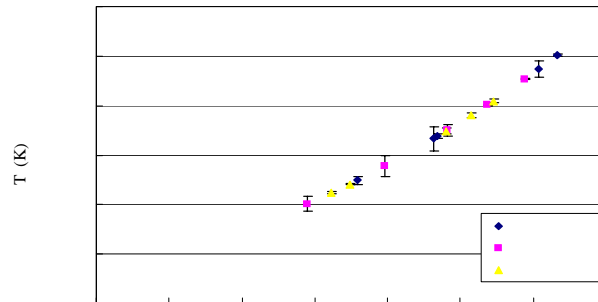


Fig. 9 Temperatures behind reflected shock wave T_5 as a function of Mach number.